Tunable Mie Scattering from Electrodeposited Cu_2O Nanoparticles

T. S. Gershon, N. N. Lal, J. J. Baumberg and J. L. MacManus-Driscoll

J. Electrochem. Soc. 2012, Volume 159, Issue 12, Pages D747-D749.
doi: 10.1149/2.069212jes

Journal of The Electrochemical Society, **159** (12) D747-D749 (2012)
0013-4651/2012/159(12)/D747/3/$28.00 © The Electrochemical Society

Tunable Mie Scattering from Electrodeposited Cu_2O Nanoparticles

T. S. Gershon,[a,z] N. N. Lal,[b] J. J. Baumberg,[b] and J. L. MacManus-Driscoll[a]

[a]*Materials Science Department, University of Cambridge, Cambridge CB2 3QZ, United Kingdom*
[b]*Physics Department, University of Cambridge, Cambridge CB3 0HE, United Kingdom*

Mie scattering centers comprised of high-refractive-index Cu_2O are prepared using a rapid one-step electrodeposition procedure. The deposition of cubic nanoparticles is facilitated by a high-pH precursor solution, which allows for low Cu_2O nucleation density and large grain size. The scattering resonant frequency and peak width are easily tuned across the visible spectrum by controlling the pH of the electrochemical solution and the duration and rate of deposition.
 [DOI: 10.1149/2.069212jes]

Manuscript submitted June 29, 2012; revised manuscript received September 23, 2012. Published October 20, 2012.

In recent years increasing attention has been devoted to reproducing the structural coloration found in nature by assembling inorganic building blocks into complex nanostructures.[1–3] Structural coloration in inorganic films can result from photonic crystal behavior, as in the butterfly wing or the scarab beetle, or from Mie scattering centers with high refractive index. The preparation of inorganic Mie scattering centers has been demonstrated with various materials including ZnS, ZnSe, and TiO_2.[4–6] Dielectric scatterers can be used to enhance optical effects in solar cells and other optoelectronic devices.[7–10]

Cu_2O ($n \sim 3$)[11] is an attractive candidate material for a broad range of optoelectronic applications and is readily processed via a simple aqueous electrodeposition route.[12–14] Previous efforts to prepare Cu_2O scattering centers via solution routes resulted in nanoparticle aggregates with non-uniform spatial distributions.[15] In the present work, spatially-uniform films of Mie-scattering centers comprised of Cu_2O are prepared using a rapid low-temperature aqueous electrodeposition procedure. The optical properties of these cubic nanoparticle films can be finely tuned by altering the rate and duration of the depositions.

Experimental

Commercial ITO substrates (<10 Ω/sq) were cleaned using Savona soap, deionized water, and sonication in acetone and isopropanol for 10 min each. An aqueous solution was prepared containing 0.4 M copper sulfate and 3 M lactic acid as per Ref. 16. The pH of the solution (at 40°C) was adjusted by adding 4 M aqueous NaOH until the desired pH was achieved, as measured with an Oakton pH meter and probe. Galvanostatic deposition was carried out at −1 and −0.5 mA/cm^2 with a Pt counter electrode to examine particle dependence on deposition rate.

Optical density measurements were performed using an HP UV-VIS spectrometer in transmission mode. High-resolution top-down SEM images were acquired on a LEO VP-1530 field emission microscope under a 10 kV beam. Analysis of SEM images was performed using ImageJ software. Particle "radius" is defined as the radius of a sphere containing the same volume as the average cubic particle in a given film.

Results and Discussion

Cu_2O films prepared at pH values of 10, 11, and 12 display significantly different microstructures (Figure 1a–1c). All three samples in Figure 1 were prepared using an identical current density (−1 mA/cm^2) and deposition time (two minutes). Higher pH values give larger-grained material while lower pH gives dense, conformal films.[12,13] The solution pH also influences Cu_2O nucleation density. This could be due to the pH-dependence of the reduction potential[17] and/or the coordination between copper ions and lactate in solution, both of which affect the driving force for Cu_2O nucleation.

The microstructural differences strongly influence the way these films interact with light (Figure 1d). While the dense samples prepared at pH values of 10 and 11 show the characteristic optical density profile of Cu_2O ($E_g \sim 2.0$ eV, with a direct-forbidden to direct-allowed transition at 2.6 eV), the sample prepared at a pH of 12 shows additional scattering peaks at wavelengths not absorbed by Cu_2O.[11] These peaks are the result of Mie scattering, which arises when the dielectric particle size is comparable to the wavelength of incident light.[18,19] It is noted that the optical density of the pH = 12 sample at short wavelengths ($E > E_g$) is lower than that of the other samples; the increased transmission at these wavelengths is likely due to disconcontinuities in the film. The solution pH is fixed at 12 in the remainder of this study to preserve the characteristic Mie scattering peaks.

The size of electrodeposited Cu_2O nanoparticles is easily controlled by altering the deposition duration (Figure 2). As the particle size increases, the position of the sub-bandgap peak in the UV-VIS pattern red-shifts in accordance with Mie theory (Figure 3a–3c).[18,19] The predicted position of the highest-energy Mie peak for spherical Cu_2O particles embedded in an n = 1.8 dielectric shows close

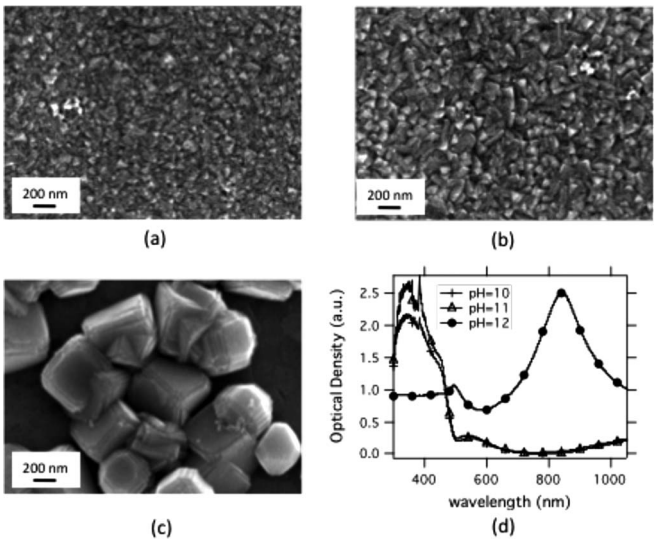

Figure 1. High-resolution SEM images of Cu_2O films (−1 mA/cm^2) deposited for two minutes using pH values of (a) 10, (b) 11, and (c) 12. (d) Optical density profiles of the Cu_2O films in (a-c), taken in transmission mode. Symbols are used to distinguish samples when printed in black and white.

[z]E-mail: talia.gershon@gmail.com

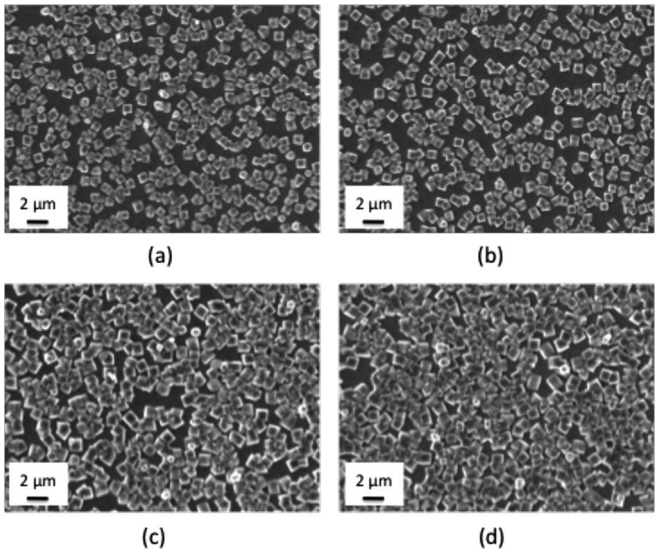

Figure 2. (a) Top-down SEM images of Cu_2O nanoparticles electrodeposited (pH = 12, −1 mA/cm^2) for different times: (a) 2 min, (b) 3 min, (c) 4 min, and (d) 5 min.

agreement with experiment as particle size increases (Figure 3b). Mie exctinction spectra are calculated using analytical code written in Igor (Wavemetrics) and literature values of the Cu_2O extinction spectra.[11] The choice of n = 1.8 accounts for the ITO-coated substrate (n∼1.8),[20] the proximity of high-n neighboring particles, and the resonance shift associated with non-spherical compared to spherical particles.[21] A requirement for Mie scattering is homogeneity of particle size in a given

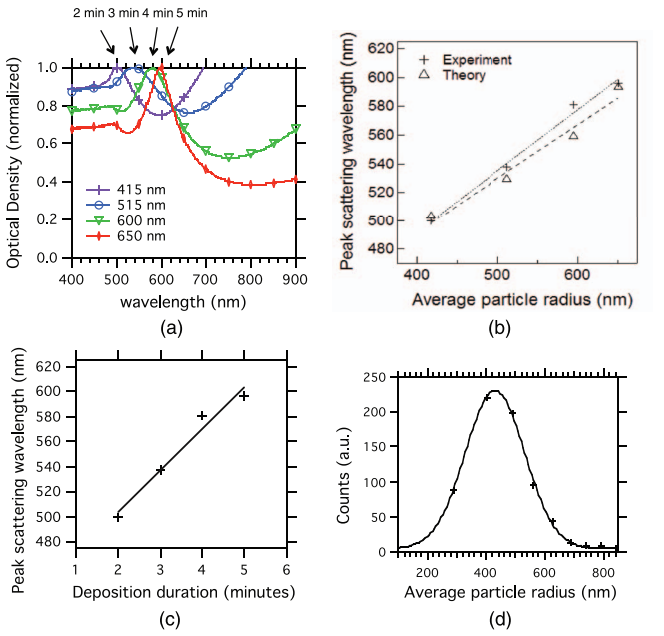

Figure 3. (a) Normalized optical density spectra of Cu_2O films deposited at −1 mA/cm^2 for different durations of time (pH = 12). The average particle radius is given. Symbols are used to distinguish samples when printed in black and white. (b) Experimental and theoretical position of optical density peak with respect to average Cu_2O nanoparticle effective radius. (c) Position of optical density peak with respect to deposition time (−1 mA/cm^2, pH = 12). (d) Distribution of nanoparticle radii in a sample prepared at pH = 12 and using a deposition rate of −1 mA/cm^2 and duration of two minutes. The SEM image analyzed was approximately 40 μm x 25 μm. Markers in (b)-(d) represent data points.

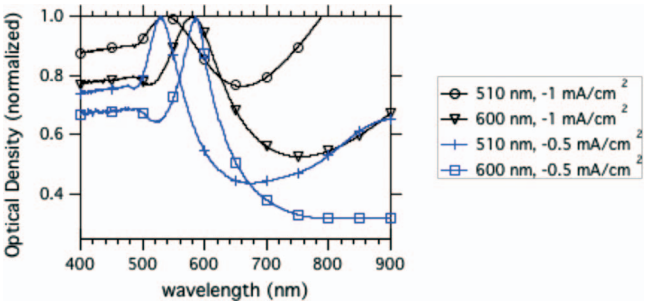

Figure 4. Normalized optical density patterns of Cu_2O nanoparticle films deposited at −1 mA/cm^2 for 3 min (rad ∼ 510 nm) or 4 min (rad ∼ 600 nm) and −0.5 mA/cm^2 for 7 min (rad ∼ 510 nm) or 10 min (rad ∼ 600 nm). All samples were deposited at a pH value of 12. Symbols are used to distinguish samples when printed in black and white.

film; Figure 3d shows the distribution of nanoparticle sizes in the sample prepared at a pH of 12 using a deposition rate of −1 mA/cm^2 and duration of two minutes. The distribution is well fit by a Gaussian curve.

It is noted that two separate peaks appear over the wavelength range probed (Figure 1d). Both of these peaks follow the spectral dependence described above. Additionally, continuous films of Cu_2O (∼200-nm thick films prepared at pH = 10, 11 and 1-μm-thick films prepared at pH = 12) do not exhibit these long-wavelength optical density peaks. Therefore, the possibility of long-wavelength defect absorption is excluded. Both peaks are thus the result of Mie scattering.

We are also able to control the width of the scattering peak by adjusting the rate of the deposition. Films grown at the same pH (12) but at a lower current density (−0.5 mA/cm^2, as opposed to −1 mA/cm^2) scatter more strongly and with narrower linewidth (by a factor of ∼2 FWHM) (Figure 4). High-resolution SEM images of these samples are shown in Figure 5. Slower deposition rates lead to an increase in particle density, particle uniformity, and the sharpness of the particle edges and corners.

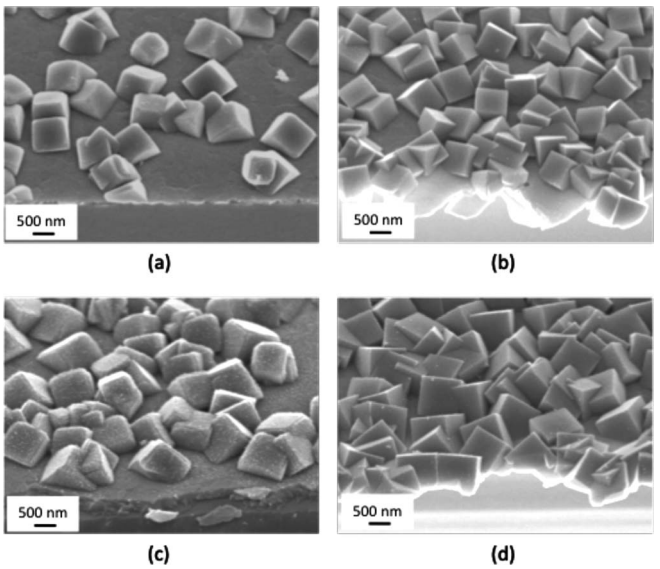

Figure 5. High-resolution cross-sectional SEM images (45 degrees) of nanoparticle films prepared using pH = 12 solution and current densities of −1 mA/cm^2 (a, c) or −0.5 mA/cm^2 (b, d). Average particle radii were 510 nm (a, b) and 600 nm (c, d).

Conclusions

In conclusion, a rapid one-step aqueous electrodeposition process can be used to prepare cubic Mie scattering centers comprised of Cu_2O. The pH of the processing solution determines whether the deposited film is dense and homogeneous (pH = 10, 11) or sparsely-populated with nanoparticles (pH = 12). The position, magnitude, and line-width of the resonant scattering frequency is readily controlled via deposition rate and duration. This work is applicable in a wide range of optoelectronic applications in which high-refractive-index scattering centers can be used to improve performance.

Acknowledgments

The authors would like to thank Dr. M. Hawkeye for the development of the Mie code. Additionally, the authors are grateful to the Gates Cambridge Trust, the ERC Advanced Investigator grant, NOVOX, ERC-2009-adG 247276 and EPSRC EP/G060649/1 for funding this work.

References

1. A. R. Parker and H. E. Townley, *Nat. Nanotechnol.*, **2**, 347 (2007).
2. K. Michielsen and D. G. Stavenga, *J. R. Soc. Interface*, **5**, 85 (2008).
3. A. E. Seago, P. Brady, J.-P. Vigneron, and T. D. Schults, *J. R. Soc. Interface*, **6**, S165 (2009).
4. M. Scholz, R. Vacassy, J. Dutta, and H. Hofmann, *J. Appl. Phys.*, **83**, 7860 (1998).
5. M.-C. Tsai, T.-L. Tsai, D.-B. Shieh, H.-T. Chiu, and C.-Y. Lee, *Anal. Chem.*, **81**, 7590 (2009).
6. H. Zhong, Z. Wei, M. Ye, Y. Yan, Y. Zhou, Y. Ding, C. Yang, C. Yang, and Y. Li, *Langmuir*, **23**, 9008 (2007).
7. S. Hore, C. Better, R. Kern, H. Smit, and A. Hinsch, *Sol. Energ. Mat. Sol. C.*, **90**, 1176 (2006).
8. H.-J. Koo, J. Park, B. Yoo, K. Yoo, K. Kim, and N.-G. Park, *Inorg. Chim. Acta*, **361**, 677 (2008).
9. J. R. Nagel and M. A. Scarpulla, *Opt. Express*, **18**, A139 (2010).
10. C. K. Huang, H. H. Lin, J. Y. Chen, K. W. Sun, and W.-L. Chang, *Sol. Energ. Mat. Sol. C.*, **95**, 2540 (2011)
11. C. Malerba, F. Biccari, C. L. A. Ricardo, M. D'Incau, P. Scardi, and A. Mittiga, *Sol. Energ. Mat. Sol. C.*, **95**, 2848 (2011).
12. Y. C. Zhou and Y. A. Switzer, *Mater. Res. Innov.*, **2**, 22 (1998).
13. Y. Zhou and J. A. Switzer, *Scripta Mater.*, **38**, 1731 (1998).
14. P. E. de Jongh, D. Vanmaekelbergh, and J. J. Kelly, *Chem. Mater.*, **11**, 3512 (1999).
15. P. McFayden and E. Matijevic, *J. Colloid Interf. Sci.*, **44**, 95 (1973).
16. K. Mizuno, M. Izaki, K. Murase, T. Shinagawa, M. Chigane, M. Inaba, A. Tasaka, and Y. Awakura, *J. Electrochem. Soc.*, **152**, C179 (2005).
17. C. D. Lokhande and S. H. Pawar, *Phys. Status Solidi. A*, **111**, 17 (1989).
18. C. F. Bohren and D. R. Huffman, *Absorption and scattering of light by small particles*, John Wiley & Sons, New York (1983).
19. H. C. van de Hulst, *Light scattering by small particles*, Dover Publications, Inc., New York (1957).
20. http://www.stanford.edu/group/mcgehee/transfermatrix/.
21. M. I. Mishchenko, J. W. Hovenier, and L. D. Travis editors, *Light Scattering by Nonspherical Particles*, Academic Press, Florida (1999).